RESEARCH ARTICLE

WILEY

Cross-cohort replicable resting-state functional connectivity in predicting symptoms and cognition of schizophrenia

Chunzhi Zhao[1,2] | **Rongtao Jiang**[3] | **Juan Bustillo**[4] | **Peter Kochunov**[5] |
Jessica A. Turner[6] | **Chuang Liang**[1,2] | **Zening Fu**[6] | **Daoqiang Zhang**[1,2] |
Shile Qi[1,2] | **Vince D. Calhoun**[6]

[1]College of Computer Science and Technology, Nanjing University of Aeronautics and Astronautics, Nanjing, China

[2]Key Laboratory of Brain-Machine Intelligence Technology, Ministry of Education, Nanjing University of Aeronautics and Astronautics, Nanjing, China

[3]Department of Radiology and Biomedical Imaging, Yale School of Medicine, New Haven, Connecticut, USA

[4]Department of Psychiatry and Behavioral Sciences, University of New Mexico, Albuquerque, New Mexico, USA

[5]Department of Psychiatry and Behavioral Sciences, University of Texas Health Science Center Houston, Houston, Texas, USA

[6]Tri-institutional Center for Translational Research in Neuroimaging and Data Science (TReNDS) Georgia State University, Georgia Institute of Technology, Emory University, Atlanta, Georgia, USA

Correspondence
Rongtao Jiang, Department of Radiology and Biomedical Imaging, Yale School of Medicine, New Haven, CT, USA.
Email: rongtao.jiang@yale.edu

Shile Qi, Nanjing University of Aeronautics and Astronautics, Nanjing, China.
Email: shile.qi@nuaa.edu.cn

Abstract

Schizophrenia (SZ) is a debilitating mental illness characterized by adolescence or early adulthood onset of psychosis, positive and negative symptoms, as well as cognitive impairments. Despite a plethora of studies leveraging functional connectivity (FC) from functional magnetic resonance imaging (fMRI) to predict symptoms and cognitive impairments of SZ, the findings have exhibited great heterogeneity. We aimed to identify congruous and replicable connectivity patterns capable of predicting positive and negative symptoms as well as cognitive impairments in SZ. Predictable functional connections (FCs) were identified by employing an individualized prediction model, whose replicability was further evaluated across three independent cohorts (BSNIP, SZ = 174; COBRE, SZ = 100; FBIRN, SZ = 161). Across cohorts, we observed that altered FCs in frontal-temporal-cingulate-thalamic network were replicable in prediction of positive symptoms, while sensorimotor network was predictive of negative symptoms. Temporal-parahippocampal network was consistently identified to be associated with reduced cognitive function. These replicable 23 FCs effectively distinguished SZ from healthy controls (HC) across three cohorts (82.7%, 90.2%, and 86.1%). Furthermore, models built using these replicable FCs showed comparable accuracies to those built using the whole-brain features in predicting symptoms/cognition of SZ across the three cohorts ($r = .17$–$.33$, $p < .05$). Overall, our findings provide new insights into the neural underpinnings of SZ

Chunzhi Zhao and Rongtao Jiang contributed equally to this work.

symptoms/cognition and offer potential targets for further research and possible clinical interventions.

KEYWORDS

cognition, fMRI, functional connectivity, positive/negative symptoms, prediction, schizophrenia

1 | INTRODUCTION

Schizophrenia (SZ) is a chronic and disabling mental illness that affects approximately 1% of the world's population (Cai et al., 2024; Kraguljac et al., 2021; Liang et al., 2023; Tang et al., 2012). It is characterized by the adolescence-to-young adulthood, onset of symptoms that include psychosis, disorganized thoughts, apathy and cognitive decline (Zheng et al., 2021). The core symptoms of SZ can be separated into positive (including delusions, hallucinations, disordered thinking, and disorganized behavior) and negative symptoms (including impaired motivation, reduction in affect and spontaneous speech, and social withdrawal). Cognitive impairments in SZ involve deficits in attention, memory, learning, and executive function (Joyce & Roiser, 2007; Qi et al., 2020; S. Qi et al., 2021; Rodrigues-Amorim et al., 2017; Wang et al., 2020). Advances in neuroimaging techniques, especially resting-state functional MRI (rs-fMRI), have led to compelling insights into human brain function of SZ (Raimondo et al., 2021; Zhao et al., 2022). Moreover, the integration of brain imaging and machine learning models has significantly contributed to the understanding of functional alterations that occur in the brain of individuals with SZ (Berman et al., 2016; de Filippis et al., 2019; L. Fan et al., 2021; Qiu et al., 2021; Xi et al., 2021). Although previous studies utilizing rs-fMRI have demonstrated extensive patterns of abnormal brain connectivity in SZ (Baker et al., 2014; Dong et al., 2018; Mwansisya et al., 2017; Skudlarski et al., 2010), the identification of replicable abnormal connectivity patterns related to symptoms and cognitive dimensions remains elusive (Adhikari et al., 2019; Elliott et al., 2021; Guo et al., 2023).

Numerous studies have reported inconsistent or diverging results regarding rs-fMRI based prediction of positive/negative symptoms and cognitive impairments in SZ. A study revealed that between-network connections of the frontoparietal control network (FPN) were found to contribute the most in predicting the positive symptoms (Y.-S. Fan et al., 2022), while a combination of between-network connections of the default mode network, FPN, and within-network connections of the FPN significantly contributed to the prediction of negative symptoms. Another study indicated that connections contributing to the positive symptoms were predominantly those between the FPN, dorsal attention network, and sensorimotor network, while connections contributing to the negative symptoms mainly involved the FPN, sensorimotor network, and the salience network (Wang et al., 2020). A research discovered that connections from the left hippocampus to the left inferior parietal sulcus, as well as connections from the right hippocampus to the left hippocampus, were predictive of positive symptoms (Uscătescu et al., 2021).

Additionally, connections originating from the left hippocampus to the dorsal anterior cingulate cortex, left inferior parietal sulcus, and right hippocampus were predictive of negative symptoms. Researchers have discovered that cognitive impairments of SZ were related to decreased prefrontal-thalamic connectivity and increased sensorimotor-thalamic connectivity (P. Chen et al., 2019). Another research found that the connectivity between the medial prefrontal and temporal regions predicted cognitive impairments (Abram et al., 2017). These inconsistent findings may be due to the heterogeneity in sample characteristics (i.e., heterogeneity in patient populations and pharmacologic effects) and technical issues (i.e., differences in hardware, scanning and analytic protocols) (J. Chen et al., 2021). Furthermore, these studies predominantly focused on examining group-level correlations between symptoms and brain measurements instead of making prediction of core symptoms on a subject level. Finally, none of these studies have examined replication of findings in independent samples. In light of this, identifying reproducible and stable connectivity patterns to predict positive/negative symptoms or cognitive impairments in SZ appears particularly necessary.

In this study, we aim to identify replicable and consistent connectivity patterns that can predict positive/negative symptoms and cognitive impairments in SZ. Specifically, we first constructed an individualized model to predict the positive/negative symptoms and cognitive impairments across three cohorts. This model combines feature selection and machine learning and has been previously employed to predict cognitive domain scores, symptoms severity, and personality traits (Beaty et al., 2018; Feng et al., 2022; Jiang, Calhoun, et al., 2020; Jiang, Zuo, et al., 2020; Shen et al., 2017). Second, in order to identify stable and consistent functional connections (FCs), we conducted a statistical analysis of the reproducible FCs among the top 80% features in the prediction model for each symptom set. Finally, we employed a back-propagation neural network (BPNN) to verify the diagnostic ability of the identified replicable FCs on the three cohorts (Liang et al., 2023). We also used the overlapping FCs in any two cohorts to predict the corresponding symptoms in the third cohort. Eventually, we identified replicable FCs that effectively predict positive and negative symptoms as well as cognitive impairments in SZ.

2 | MATERIALS AND METHODS

2.1 | Participants in three independent cohorts

Three independent sites contributed a total of 901 subjects in this study, including 435 SZ patients (BSNIP [Bipolar and Schizophrenia

TABLE 1 Demographic and clinical information.

Cohorts	BSNIP			COBRE			FBIRN		
	SZ	HC	*p*	SZ	HC	*p*	SZ	HC	*p*
Number	$n = 174$	$n = 219$	NA	$n = 100$	$n = 90$	NA	$n = 161$	$n = 157$	NA
Age	34.5 ± 12.1	38.8 ± 12.6	5.8e−04	38.5 ± 14.1	38.0 ± 11.6	.8	39.0 ± 11.3	37.5 ± 11.3	.2
Gender (M/F)	120/54	90/129	2.2e−08	78/22	65/25	.4	120/41	112/45	.5
PANSS_Positive	16.4 ± 5.7	NA	NA	15.0 ± 4.6	NA	NA	14.4 ± 5.6	NA	NA
PANSS_Negative	16.3 ± 6.1	NA	NA	14.6 ± 5.2	NA	NA	15.5 ± 5.1	NA	NA
Cognition	−1.7 ± 1.4	0.01 ± 1.1	4.5e−34	32.7 ± 12.9	49.9 ± 8.7	2.7e−19	−1.6 ± 1.3	0.01 ± 1.0	3.2e−28

Note: *p* value for two-sample *t* test among age, gender and cognition between SZ and HC.
Abbreviation: M/F, male/female.

Network for Intermediate Phenotypes]: SZ = 174; COBRE [Center for Biomedical Research Excellence]: SZ = 100; FBIRN [Functional Imaging Biomedical Informatics Research Network]: SZ = 161), and 466 healthy controls (HC) (BSNIP: HC = 219; COBRE: HC = 90; FBIRN: HC = 157). The demographic and symptomatic information are listed in Table 1. Symptoms were assessed using the Positive and Negative Symptom Scale of Psychotic Symptom Severity (PANSS) (Kay et al., 1987), and cognitive performance was measured using three different cognitive batteries. BSNIP: Brief Assessment of Cognition in SZ, BACS; FBIRN: Computerized Multiphasic Interactive Neuro-cognitive System, CMINDS; COBRE: Measurement and Treatment Research to Improve Cognition in SZ Consensus Cognitive Battery, MCCB (Supplementary Tables 1–3). Resting-state functional MRI scans were collected on 3T scanners for all subjects. Details on imaging parameters and preprocessing pipeline for the three cohorts can be found in Supplementary "Imaging parameters and preprocessing" section in Data S1 and Supplementary Table 4. The study was approved by the Institutional Review Board at each respective site, and written informed consent was obtained from all participants after providing a comprehensive description of the study procedure.

2.2 | Whole-brain FC extraction

For BSNIP, COBRE, and FBIRN cohorts, participants' brains were segmented into 246 regions of interest (ROIs) using the Brainnetome Atlas, which consists of 210 cortical and 36 subcortical nodes (L. Fan et al., 2016). The average time series of all voxels within each ROIs were calculated to obtain the fMRI time series for each node. Subsequently, the Pearson correlations were computed between the time courses of any two nodes and normalized to Z-scores using Fisher transformation, resulting in a 246 × 246 symmetric FC matrix for each subject (Jiang et al., 2018). The diagonal elements of each FC matrix were removed, and the lower triangular elements of the FC matrix were extracted as predictive features. Thus, each subject had a FC vector in a dimension of $(246 \times 245)/2 = 30{,}135$ (Figure 1a).

2.3 | Individualized prediction framework

Our data-driven predictive model which combines feature selection and machine learning methods has been employed to predict multiple health-related behaviors from connectivity data (Beaty et al., 2018; Feng et al., 2022; Jiang, Calhoun, et al., 2020; Jiang, Zuo, et al., 2020; Shen et al., 2017). In this study, we first employed Pearson correlation to select features showing the most significant associations with the target variable, and the optimal threshold was obtained through the grid search method. Subsequently, we utilized partial least squares regression (PLSR) to build the predictive model. PLSR is a widely used multivariate regression method in various fields such as bioinformatics, and neuroscience (Jiang et al., 2023; Jiang, Scheinost, et al., 2022; McIntosh et al., 1996; Meskaldji et al., 2016; Nguyen & Rocke, 2002). PLSR is particularly suitable when the number of predictors is relatively large compared to the available samples (Shen et al., 2017). PLSR is related to principal component analysis and multiple linear regression, essentially representing variables with a small number of latent components (Yoo et al., 2018).

We used leave-one-out cross-validation (LOOCV) to train multiple models. LOOCV maximizes the utilization of data for training and evaluation, enabling more accurate assessment of the model's performance (Jiang, Zuo, et al., 2020; Shen et al., 2017; Sun et al., 2020). In the leave-one-out loop, one subject is designated as the testing data, while the remaining *n*-1 subjects are used as the training dataset. During the training stage, we computed the Pearson correlation between each symptom set and each of the 30,135 connectivity features in the FC matrix. We obtained the *r* and *p* values between each feature and the respective symptoms (Abubacker et al., 2014; Sun et al., 2020). Subsequently, we designated the features that satisfied $r > 0$ and $p <$ the positive threshold as positive features. Similarly, features that satisfied $r < 0$ and $p <$ the negative threshold were designated as negative features. The optimal positive and negative thresholds were determined within the range of 0.001–0.05. Finally, all positive and negative features were put into the PLSR model as selected features. The optimal number of latent components was determined using a nested LOOCV. The parameter was tested within the range of 1–20, and
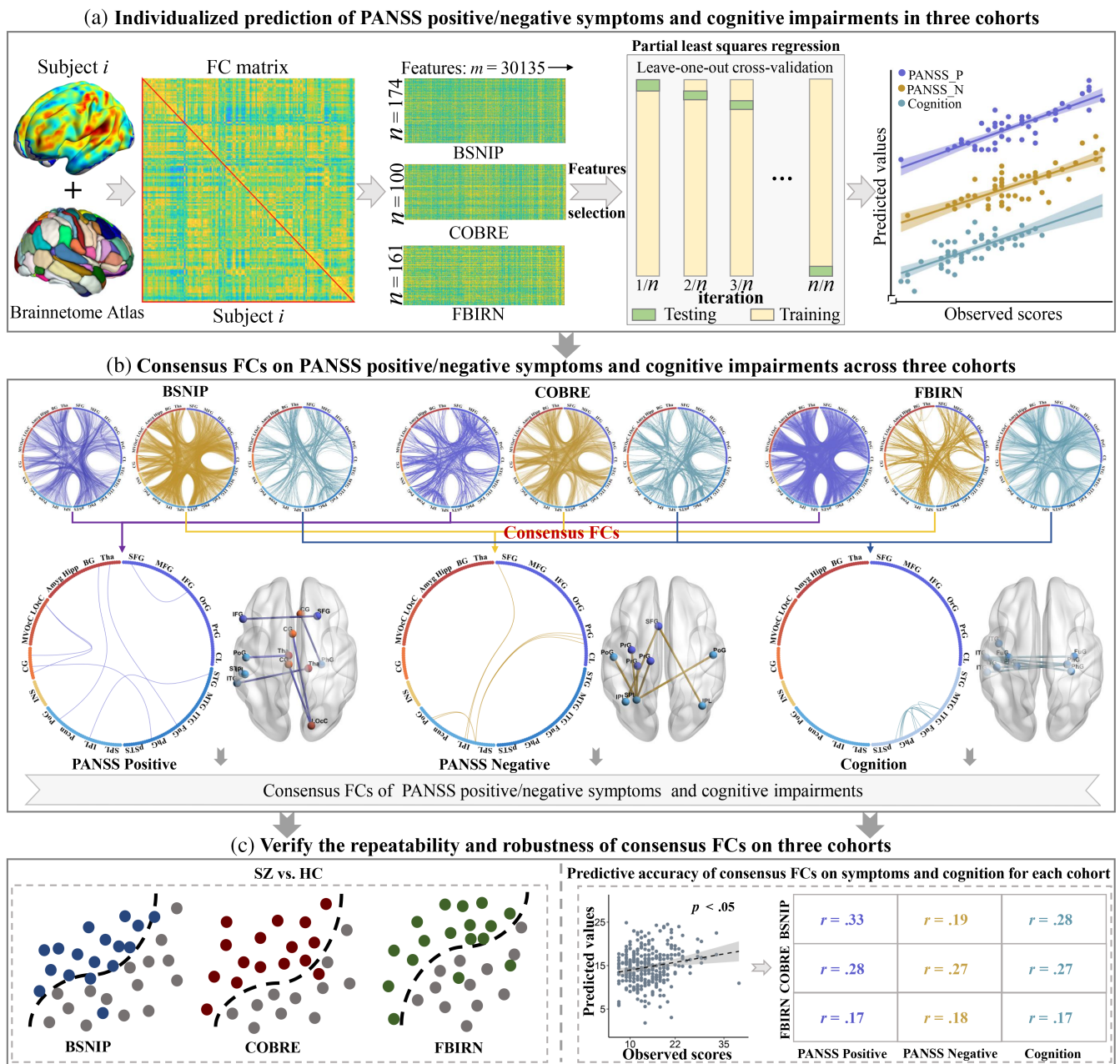
FIGURE 1 Analysis framework for this study. (a) Constructing the FC matrix for each cohort using the Brainnetome Atlas. Feature selection and PLSR were employed to build an individualized prediction model, which underwent testing using LOOCV on all subjects. Individualized prediction of positive/negative symptoms and cognitive impairments of SZ on each cohort. (PANSS_P: PANSS Positive; PANSS_N: PANSS Negative). (b) The top 80% contributing features in each prediction model were extracted, followed by overlaying them for the same symptoms across the three cohorts to identify the consistent FCs. (c) Consensus FCs were used to classify SZ and HC (left) and predict positive/negative symptoms, and cognitive impairments in each cohort (right).

the value that yielded the highest prediction accuracy was determined as the optimum number of components. In our experiments, the optimal number of latent components ranged from 3 to 10 for most conditions. Setting the parameter value too small made it difficult to model brain–behavior relationships, while setting it too large may lead to overfitting, resulting in higher prediction accuracy for the training sample but poorer generalization to the test sample (Jiang, Zuo, et al., 2020). This process was repeated n times (equal to

the number of subjects) to test all subjects. Figure 1a illustrates the prediction framework employed in this study.

2.4 | Extracting consensus FCs

In LOOCV loop, after determining the optimal number of potential components, we extracted features with higher contribution based on
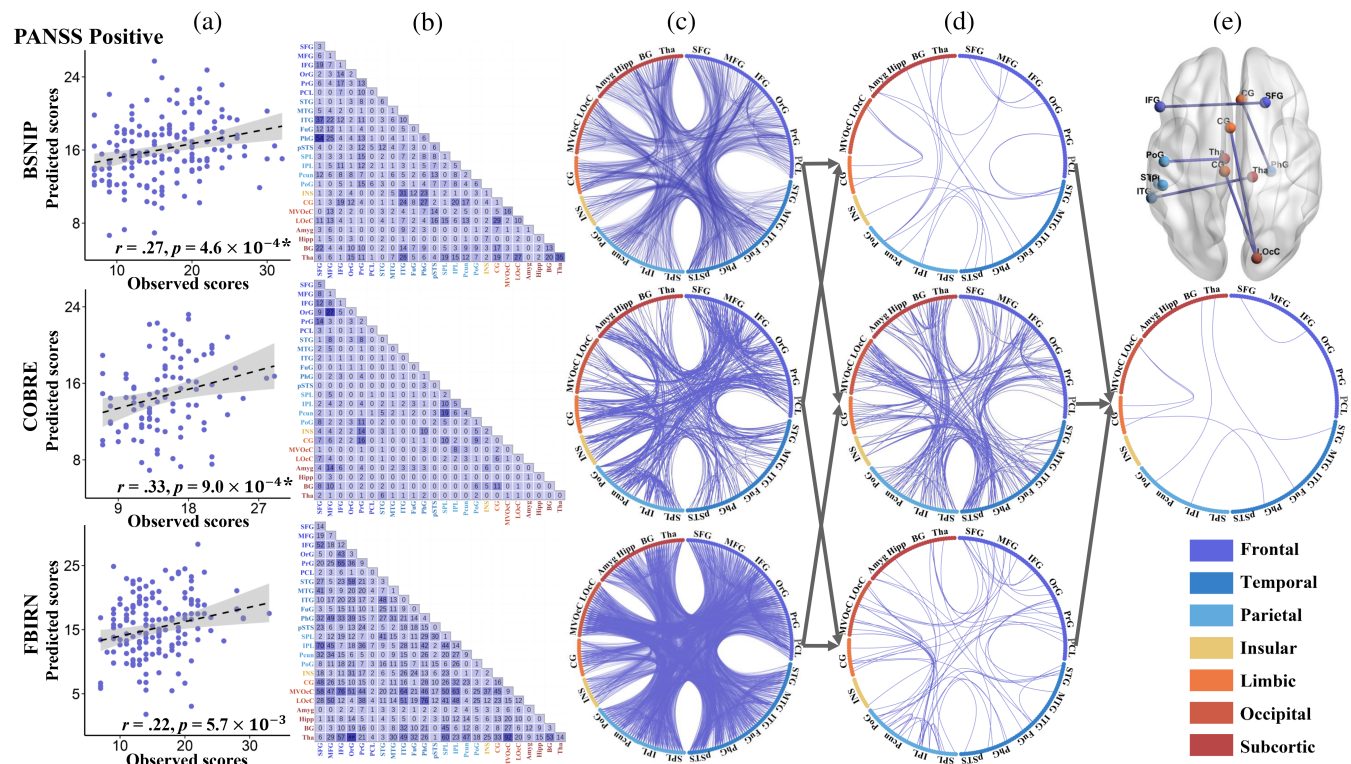
FIGURE 2 The prediction results for the positive symptoms in three cohorts. (a) Scatter plots showing model-predicted and actual scores for positive symptoms in each cohort. (b and c) Distribution of the top 80% features contributing to predicting the positive symptoms. (d) Overlay of the FCs from any two cohorts. (e) Overlay of the FC features consistently identified across the three cohorts.

the regression weight coefficients (Liu & Li, 2017). To identify the most important FCs for each symptom across the three cohorts, we extracted the top 80% features that contribute to the prediction model. Since we selected features that exhibit a high correlation with the predicted symptoms, the number of features involved in predicting symptoms were smaller. This process was performed for positive/negative symptoms and cognition impairments in the three cohorts, respectively. Within the same symptom set, we identified the features that consistently appeared across the three cohorts, which were defined as the consensus FCs for that particular symptom set (Jiang, Woo, et al., 2022) (Figure 1b).

2.5 | Repeatability and robustness of the consensus FCs

To verify the repeatability and robustness of the consensus FCs discovered for each symptom set, we conducted the following experiments. (1) The consensus FCs obtained for predicting positive/negative symptoms and cognitive impairments were combined in SZ. We used the BPNN classification model, which has proven successful in distinguishing among SZ, schizoaffective disorder, psychotic bipolar disorder and HC (Liang et al., 2023), to classify SZ and HC in each cohort (Figure 1c, left). (2) For the three cohorts, we utilized the consensus FCs associated with each symptom set as the foundation and applied the previously established predictive

framework to predict the corresponding symptoms once again (Figure 1c, right).

3 | RESULTS

3.1 | Consensus FCs in predicting the positive symptoms

Figure 2 depicts the prediction results for the positive symptoms and the consensus FCs consistently predicting positive symptoms across the three cohorts. Specifically, significant correlations were observed between model-predicted and actual clinical scores, with a Pearson correlation of $r = .27$ ($p = 4.6 \times 10^{-4*}$), $r = .33$ ($p = 9.0 \times 10^{-4*}$), and $r = .22$ ($p = 5.7 \times 10^{-3}$) for BSNIP, COBRE and FBIRN cohorts, respectively (Figure 2a). (*) indicates statistical significance after 1000 permutation testing (Supplementary "Permutation test" section in Data S1). Furthermore, the features showing the top 80% highest contributions to the prediction model of positive symptoms in each cohort were extracted (Figure 2b,c). Figure 2d illustrates the overlapping FCs consistently identified by any two cohorts. Seven FCs were consistently identified as the consensus features across three cohorts, namely: left inferior frontal gyrus (33) and right superior frontal gyrus (4); left inferior parietal lobule (137) and left superior temporal gyrus (71); right thalamus (242) and left lateral inferior temporal gyrus (99); right cingulate gyrus (180) and right parahippocampal gyrus (112); left
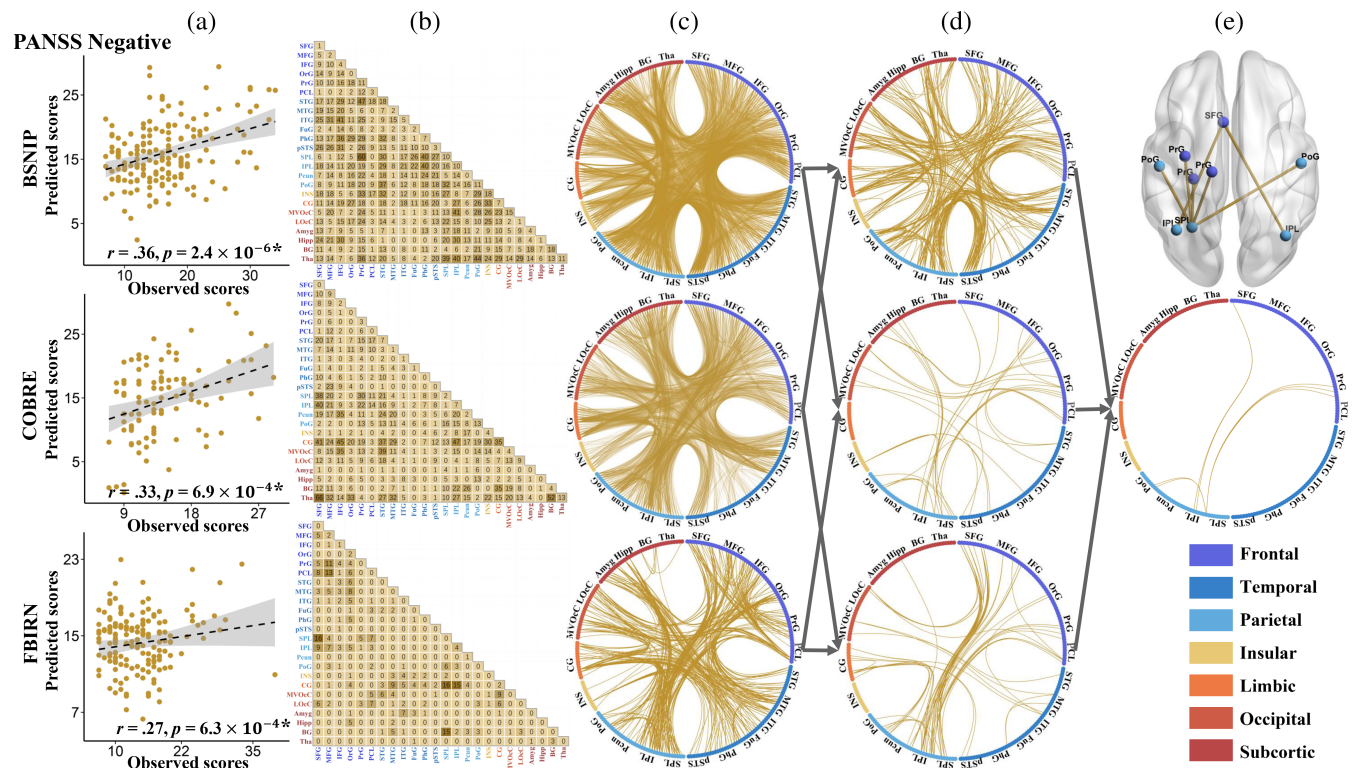
FIGURE 3 The prediction results for the negative symptoms in three cohorts. (a) Scatter plots showing model-predicted and actual scores for negative symptoms in each cohort. (b and c) Distribution of the top 80% features contributing to predicting the negative symptoms. (d) Overlay of the FCs from any two cohorts. (e) Overlay of the FCs consistently identified across the three cohorts.

thalamus (237) and left postcentral gyrus (55); and right lateral occipital cortex (208) and left cingulate gyrus (177, 185) (Figure 2e). Numbers in parentheses indicate the labeling of individual FCs corresponding to Brainnetome Atlas delineated brain regions (Supplementary Tables 5 and 6). These consensus FCs were primarily distributed among a frontal-temporal-cingulate-thalamic network.

3.2 | Consensus FCs in predicting the negative symptoms

Figure 3 illustrates the prediction results for the negative symptoms and the consensus FCs consistently predicting negative symptoms across the three cohorts. Specifically, significant correlations were observed between model-predicted and actual clinical scores, with a Pearson correlation of $r = .36$ ($p = 2.4 \times 10^{-6}$*), $r = .33$ ($p = 6.9 \times 10^{-4}$*), and $r = .27$ ($p = 6.3 \times 10^{-4}$*) for BSNIP, COBRE, and FBIRN cohorts, respectively (Figure 3a). Additionally, the features showing the top 80% highest contributions to the prediction model of negative symptoms in each cohort (Figure 3b,c). Figure 3d visually presents the overlapping FCs observed between any two cohorts. Remarkably, seven FCs were consistently identified as consensus features across three cohorts: left superior frontal gyrus (1) and left and right inferior parietal lobule (137, 138); left superior parietal lobe (133) and left precentral gyrus (55, 57, 59); left superior

parietal lobe (133) and left and right postcentral gyrus (155, 136) (Figure 3e). These consensus FCs were predominantly localized within the sensorimotor network.

3.3 | Consensus FCs in predicting the cognitive impairments

Figure 4 depicts the prediction results for cognitive impairments and the consensus FCs consistently predicting cognitive impairments across the three cohorts. Specifically, significant correlations were observed between model-predicted and actual clinical scores, with a Pearson correlation of $r = .33$ ($p = 1.1 \times 10^{-5}$*), $r = .36$ ($p = 3.8 \times 10^{-4}$*), and $r = .34$ ($p = 2.2 \times 10^{-5}$*) for BSNIP, COBRE and FBIRN cohorts, respectively (Figure 4a). At the same time, the features showing the top 80% highest contributions to the prediction model of cognitive impairments in each cohort (Figure 4b,c). Figure 4d illustrates the overlapping FCs between any two cohorts. Overall, nine FCs were identified as consensus features across three cohorts, namely, the left inferior temporal gyrus (89) and left inferior temporal gyrus (95); left lateral inferior temporal gyrus (89, 95, 101) and right parahippocampal gyrus (112); left lateral inferior temporal gyrus (95) and right parahippocampal gyrus (114); left lateral inferior temporal gyrus (93, 95) and left parahippocampal gyrus (111); left inferior temporal gyrus
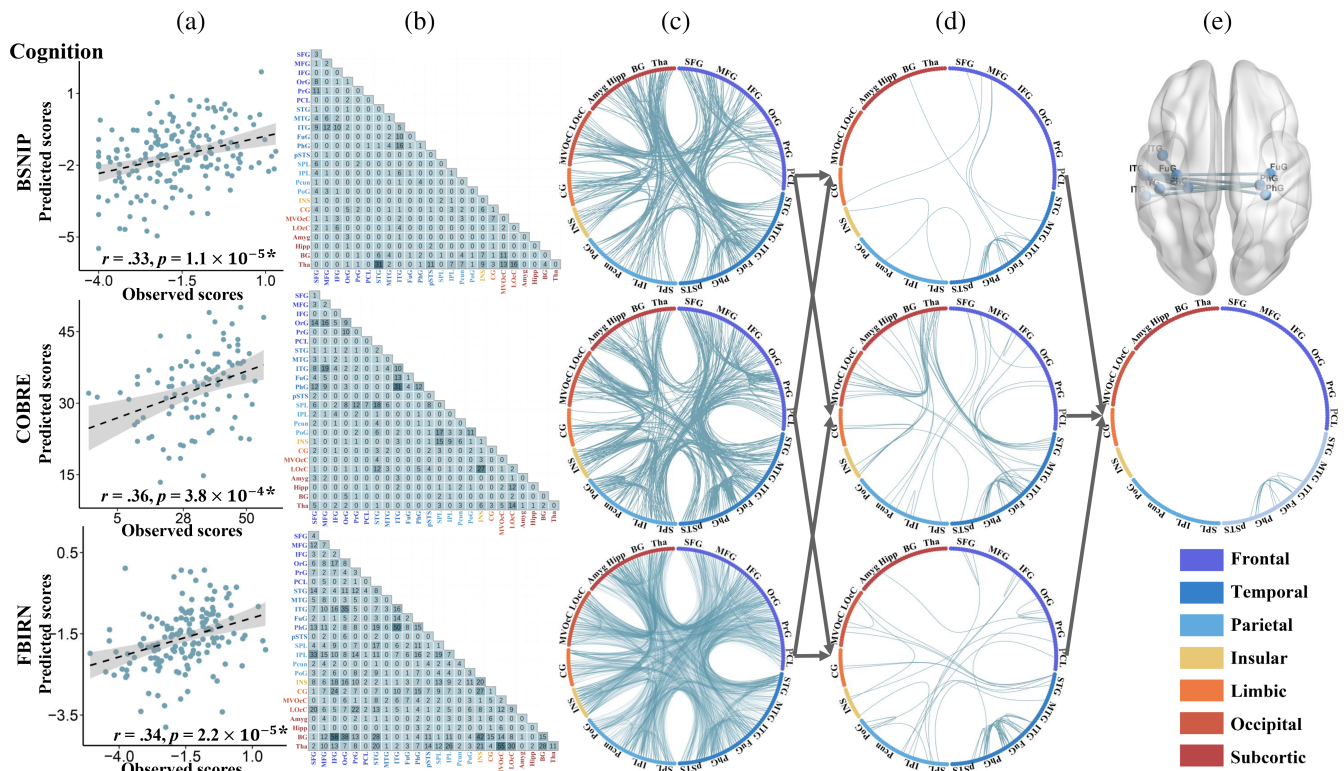
FIGURE 4 The prediction results for the cognitive impairments in three cohorts. (a) Scatter plots showing model-predicted and actual scores for cognitive impairments in each cohort. (b and c) Distribution of the top 80% features contributing to predicting the cognitive impairments. (d) Overlay of the FCs from any two cohorts. (e) Overlay of the FCs consistently identified across the three cohorts.

(95) and left and right fusiform gyrus (103, 104) (Figure 4e). These consensus FCs were primarily distributed among a temporal-parahippocampal network. Note that, we also calculated the overlap among all features (100%) in the positive/negative symptoms and cognitive prediction models across the three cohorts (Supplementary Figures 1–3). All the predicted results remain significant after excluding the influence of sites (Supplementary Figures 4 and 5).

3.4 | Robustness and reproducibility of consensus FCs

The consensus 23 FCs from each prediction model were submitted into BPNN algorithm to evaluate the classification potential between SZ and HC within each cohort. The classification accuracies between SZ and HC for BSNIP, COBRE, and FBIRN datasets were 82.7%, 90.2%, and 86.1%, respectively (Figure 5a–c). The consensus FCs for each symptom set (7, 7, 9) were used to predict the corresponding symptoms across the three cohorts to further validate the reproducibility. Models built using these replicable FCs showed comparable accuracies to those built using the whole-brain features in predicting symptoms/cognition of SZ across the three cohorts ($r = .17–.33$, $p < .05$) (Figure 5d). Furthermore, the overlapping FCs between any two cohorts can predict the corresponding symptoms in

the third cohort (Supplementary Figure 6). Finally, we counted the overlap of all features (100%) in the positive/negative symptoms and cognition prediction models. When using overlapping FCs of all features (100%) in the prediction models, the classification accuracies for BSNIP, COBRE and FBIRN were 82.8%, 91.7% and 88.4%, respectively (Supplementary Figure 7). Note that there are group differences in age and gender for BSNIP cohort. We also performed both prediction and classification after regressing out age and gender for BSNIP. Results showed that age and gender did not show a significant impact on the accuracy of classification (Supplementary Figure 8) or prediction (Supplementary Figure 9) for BSNIP cohort. The identified 23 reproducible FCs were also used to predict PANSS total for BSNIP and COBRE (PANSS total is not available for FBIRN). The prediction accuracy was $r = .38$ ($p = 3.8 \times 10^{-7}$*) for BSNIP and $r = .25$ ($p = 1.2 \times 10^{-2}$) for COBRE, respectively (Supplementary Figure 10).

4 | DISCUSSION

In this study, we successfully predicted the positive/negative symptoms and cognitive impairments in SZ using individualized prediction framework. Moreover, we identified distinct brain connectivity patterns associated with each symptom set and cognitive impairments across three cohorts. Specifically, we observed abnormal FCs in frontal-temporal-cingulate-thalamic network and sensorimotor
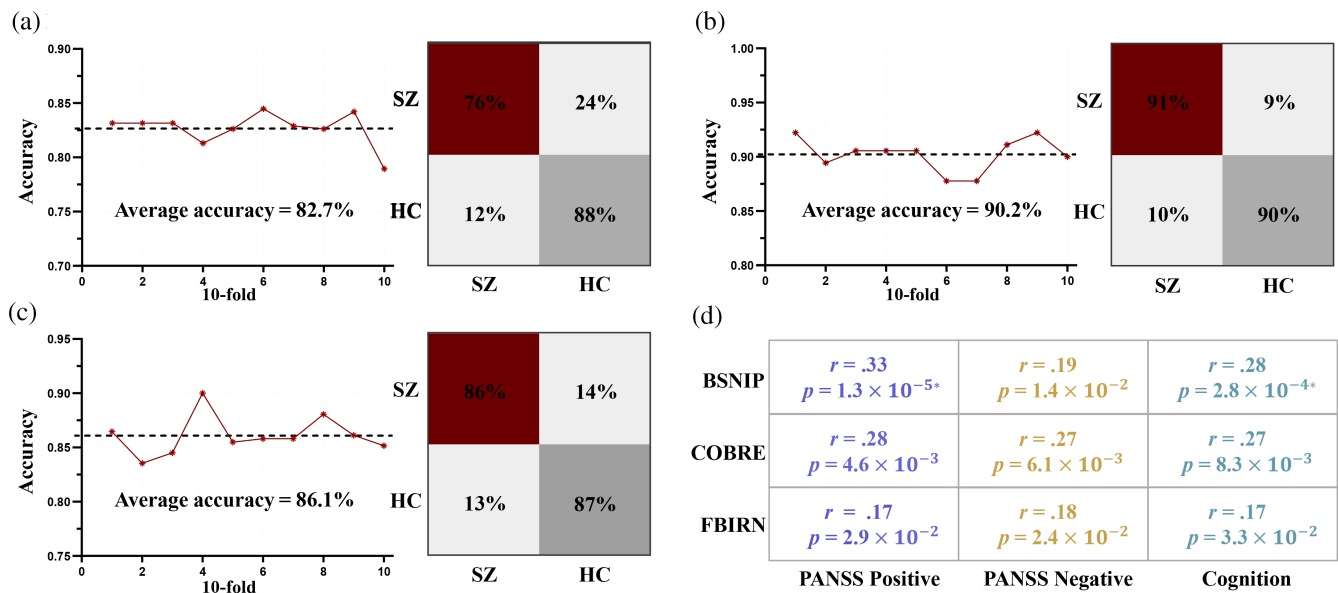
FIGURE 5 Based on the identified consensus FCs for predicting positive/negative symptoms and cognitive impairments, BPNN was used to classify SZ between HC in each cohort. Additionally, consensus FCs were employed to predict positive and negative symptoms, as well as cognitive impairments, within each cohort. (a) BSNIP: SZ versus HC. (b) COBRE: SZ versus HC. (c) FBIRN: SZ versus HC. (d) The predictive accuracy of the consensus FCs for predicting the corresponding symptoms/cognition within each cohort.

network that were replicable for positive and negative symptoms, respectively. Similarly, temporal-parahippocampal network was consistently identified in cognition prediction. These replicable FCs can successfully distinguish SZ from HC across three cohorts. More importantly, models built using these replicable FCs showed comparable accuracies to those built using the whole-brain features in predicting symptoms/cognition of SZ across the three cohorts. To the best of our knowledge, this is the first study to identify reproducible FCs that predict positive/negative symptoms and cognition in SZ through rigorous cross-cohort validation, which may more accurately reveal the abnormal FCs associated in SZ.

Our results indicated that replicable FCs used for predicting positive symptoms of SZ were primarily distributed within frontal-temporal-cingulate-thalamic network. Relevant research evidence suggested that the connectivity of the frontal, temporal, and cingulate regions was associated with the severity of positive symptoms in SZ, providing support for our findings. From a neurocircuitry perspective, aberrant interactions between the prefrontal and temporal lobes might be linked to the generation of positive symptoms in SZ (Choi et al., 2005). Specifically, abnormal connections within the frontal and temporal regions plays a crucial role in the formation of auditory hallucinations (Pettersson-Yeo et al., 2011). Additionally, significant activation of the cingulate gyrus was observed during auditory hallucinations (Silbersweig et al., 1995). Recent studies had also indicated a significant correlation between the thalamus and temporal lobe and hallucinations and delusions (Ferri et al., 2018; Kaur et al., 2020; Perez-Rando et al., 2022). Thalamic dysregulation in connectivity may have represented a core neurobiological feature of SZ, underpinning positive symptoms (Ferri et al., 2018). This aligned with the current findings of replicable connections between the thalamus

and temporal lobe in the positive symptom prediction. Therefore, this study suggests that abnormalities in connections within frontal-temporal-cingulate-thalamic network may serve as reliable FCs for predicting positive symptoms, offering valuable insights for the precise diagnosis of positive symptoms in patients with SZ.

In predicting negative symptoms of SZ, abnormal connections within sensorimotor network played a crucial role. Connections that contributed most to the estimation of negative scores in SZ mainly involved the sensorimotor regions (Wang et al., 2020), which is consistent with our findings. Frontal lobe damage has been shown to be associated with the lack of motivation and apathy (Costa et al., 2013; Y.-S. Fan et al., 2022). The aberrant connectivity between the frontal lobe and the parietal lobe is associated with symptoms of SZ, particularly negative symptoms (Brady et al., 2017; Venkataraman et al., 2012). Furthermore, the precentral gyrus is associated with anhedonia (Y. Li et al., 2018), and connections between the parietal and precentral gyrus regions may contribute to impaired motivation in SZ. The postcentral gyrus is considered to be a key structure for receiving and processing somatosensory information (H. J. Li et al., 2015), and abnormal connections between the parietal lobe and the postcentral gyrus may lead to decreased volitional behavior in the negative symptoms of SZ. In summary, the replicable FCs in predicting negative symptoms were predominantly distributed within the sensorimotor network, that hold significant potential for the investigation of negative symptoms in SZ.

Finally, FCs primarily in temporal-parahippocampal network could predict cognitive impairments in SZ. Specifically, the temporal lobe and its associated neural pathways are believed to be involved in the processing and retrieval of words and semantic knowledge (Binder et al., 2009). Connections within the temporal lobe may have complex

associations with cognitive impairments in memory and learning abilities. Aberrant connections between the parahippocampal gyrus and the temporal lobe have been identified as critical in the processes of memory encoding and retrieval (Bonnici et al., 2012; Luck et al., 2010). Therefore, connections between the parahippocampal gyrus and the temporal lobe could lead to inaccuracies in semantic comprehension and semantic memory, resulting in cognitive impairments. Furthermore, previous research has emphasized the crucial role of the fusiform gyrus in face and object recognition (Briggs et al., 2019), and connections involving these regions may play a critical role in shaping the seamless transmission and integration of visual information, contributing to the overall cognitive processing of these stimuli. In light of these factors, connections between the fusiform gyrus and the temporal lobe could impact the transmission and integration of visual information (Weiner & Grill-Spector, 2013). In summary, we found that FCs located in temporal-parahippocampal network played a crucial role in predicting cognitive impairments in SZ. These reproducible FCs have the potential to serve as a key neural circuitry foundation in the study of cognitive impairments in SZ.

The current findings of this study are further extended beyond previous FC-based prediction analyses in BSNIP, COBRE, and FBIRN cohorts. In an investigation leveraging the COBRE cohort, researchers employed a deep learning approach and identified that the cerebellum, temporal lobe, insula, and cingulate gyrus exhibited predictive capabilities for positive symptoms (Yamaguchi et al., 2021). These findings bear congruence with our observations regarding the temporal lobe and cingulate gyrus for positive symptoms. Utilizing the BSNIP, COBRE, and FBIRN cohorts, another study revealed that abnormalities within the frontotemporal network proved predictive of cognitive impairments and the severity of negative symptoms across the three cohorts (S. Qi et al., 2022). This is consistent with our finding of abnormal connections in the frontal lobe on negative symptoms, as well as abnormal temporal lobe connectivity associated with cognitive impairments. Furthermore, in a study leveraging the COBRE and FBIRN cohorts, researchers identified that irregularities in the salience network, corpus callosum, central executive, and default mode networks predicted cognitive impairments (Sui et al., 2018). These brain networks exhibit partial overlap with our findings concerning cognitive impairments in the temporal lobe and parahippocampal gyrus. Comparing with previous single cohort FC-based analyses, the current cross-cohort validated prediction offers a more rigorous and replicable characterization of symptoms/cognition-related functional architectures in SZ.

There are several limitations that should be acknowledged, which may impact the interpretation of our results. Firstly, note that the BSNIP and FBIRN cohorts utilized in our study were collected from multiple sites, each employing different MRI scanners. However, the predictive accuracy of including site as a covariate on BSNIP and FBIRN remain significant (Supplementary Figure 5), as well as for the round-robin validation by excluding one site at a time for BSNIP (Supplementary Figure 4). Secondly, the three cohorts involved chronically-ill SZ patients treated with antipsychotic medications. Antipsychotic drugs not only improve symptomatology, they can cause neuro-motoric side-effects and they affect the brain structurally and functionally (Lesh et al., 2015; Zeng et al., 2022). Hence, the FC networks identified in SZ may be confounded by medication effects on the brain. Follow-up studies in early SZ with no or minimal medication exposure are necessary. Finally, the effect sizes of prediction accuracy between model-predicted and actual scores were modest (correlations approximately .22–.36) for both symptoms and cognitive scores. Our main goal is to identify repeatable brain connection patterns among different cohorts, rather than necessarily achieving the highest prediction accuracy. Although the effect size between model-predicted and actual clinical scores was modest, models based on our identified replicable FCs achieved comparable prediction accuracy as those achieved using whole-brain connections. This suggests that the replicable FCs we found do capture meaningful individual differences related to symptoms/cognition.

In summary, using machine learning-based predictive modeling, our study identified reproducible FC patterns for positive/negative symptoms and cognitive impairments in SZ across three cohorts. We observed abnormal FCs in frontal-temporal-cingulate-thalamic network that were replicable of positive symptoms, while sensorimotor network was predictive of negative symptoms. Furthermore, the temporal-parahippocampal network was consistently identified in predicting cognition. The identified replicable FCs distinguished SZ from HC robustly across the three cohorts. More importantly, models built using these replicable FCs showed comparable accuracies to those built using the whole-brain features in predicting symptoms/cognition of SZ across the three cohorts. Overall, our findings provide new insights into the neural underpinnings of SZ symptoms/cognition and offer potential targets for further research and possible clinical interventions.

AUTHOR CONTRIBUTIONS

Shile Qi and Rongtao Jiang conceptualized the study. Chunzhi Zhao performed the data analysis and wrote the initial draft. Juan Bustillo, Peter Kochunov, Jessica A. Turner, Chuang Liang, Daoqiang Zhang, Vince D. Calhoun provided critical review of the results and paper. Zening Fu preprocessed the fMRI data for BSNIP, COBRE and FBIRN.

ACKNOWLEDGEMENTS

CONFLICT OF INTEREST STATEMENT

The authors declare no conflicts of interest.

DATA AVAILABILITY STATEMENT

The data that support the findings of this study are available on request from Prof. Calhoun. The data are not publicly available due to privacy or ethical restrictions.

ORCID

Zening Fu 🆔 https://orcid.org/0000-0002-1591-4900

REFERENCES

Abram, S. V., Wisner, K. M., Fox, J. M., Barch, D. M., Wang, L., Csernansky, J. G., MacDonald, A. W., & Smith, M. J. (2017). Fronto-temporal connectivity predicts cognitive empathy deficits and experiential negative symptoms in schizophrenia. *Human Brain Mapping*, 38 (3), 1111–1124. https://doi.org/10.1002/hbm.23439

Abubacker, N. F., Azman, A., Doraisamy, S., Azmi Murad, M. A., Elmanna, M. E. M., & Saravanan, R. (2014). Correlation-based feature selection for association rule mining in semantic annotation of mammographic medical images. *Lecture Notes in Computer Science*, 482–493. https://doi.org/10.1007/978-3-319-12844-3_41

Adhikari, B. M., Hong, L. E., Sampath, H., Chiappelli, J., Jahanshad, N., Thompson, P. M., Rowland, L. M., Calhoun, V. D., Du, X., Chen, S., & Kochunov, P. (2019). Functional network connectivity impairments and core cognitive deficits in schizophrenia. *Human Brain Mapping*, 40 (16), 4593–4605. https://doi.org/10.1002/hbm.24723

Baker, J. T., Holmes, A. J., Masters, G. A., Yeo, B. T. T., Krienen, F., Buckner, R. L., & Öngür, D. J. (2014). Disruption of cortical association networks in schizophrenia and psychotic bipolar disorder. *JAMA Psychiatry*, 71(2), 109–118. https://doi.org/10.1001/jamapsychiatry.2013.3469

Beaty, R. E., Kenett, Y. N., Christensen, A. P., Rosenberg, M. D., Benedek, M., Chen, Q., Fink, A., Qiu, J., Kwapil, T. R., Kane, M. J., & Silvia, P. J. (2018). Robust prediction of individual creative ability from brain functional connectivity. *Proceedings of the National Academy of Sciences of the United States of America*, 115(5), 1087–1092. https://doi.org/10.1073/pnas.1713532115

Berman, R. A., Gotts, S. J., McAdams, H. M., Greenstein, D., Lalonde, F., Clasen, L., Watsky, R. E., Shora, L., Ordonez, A. E., Raznahan, A., Martin, A., Gogtay, N., & Rapoport, J. (2016). Disrupted sensorimotor and social–cognitive networks underlie symptoms in childhood-onset schizophrenia. *Brain*, 139(1), 276–291. https://doi.org/10.1093/brain/awv306

Binder, J. R., Desai, R. H., Graves, W. W., & Conant, L. L. (2009). Where is the semantic system? A critical review and meta-analysis of 120 functional neuroimaging studies. *Cerebral Cortex*, 19(12), 2767–2796. https://doi.org/10.1093/cercor/bhp055

Bonnici, H. M., Kumaran, D., Chadwick, M. J., Weiskopf, N., Hassabis, D., & Maguire, E. A. (2012). Decoding representations of scenes in the medial temporal lobes. *Hippocampus*, 22(5), 1143–1153. https://doi.org/10.1002/hipo.20960

Brady, R., Tandon, N., Keshavan, M., & Ongur, D. (2017). Negative symptoms of schizophrenia and fronto-parietal circuit dysfunction. *Biological Psychiatry*, 81(10), S111. https://doi.org/10.1016/j.biopsych.2017.02.285

Briggs, R. G., Chakraborty, A. R., Anderson, C. D., Abraham, C. J., Palejwala, A. H., Conner, A. K., Pelargos, P. E., O'Donoghue, D. L., Glenn, C. A., & Sughrue, M. E. (2019). Anatomy and white matter connections of the inferior frontal gyrus. *Clinical Anatomy*, 32(4), 546–556. https://doi.org/10.1002/ca.23349

Cai, M., Ji, Y., Zhao, Q., Xue, H., Sun, Z., Wang, H., Zhang, Y., Chen, Y., Zhao, Y., Zhang, Y., Lei, M., Wang, C., Zhuo, C., Liu, N., Liu, H., & Liu, F. (2024). Homotopic functional connectivity disruptions in schizophrenia and their associated gene expression. *Neuroimage*, 289, 120551. https://doi.org/10.1016/j.neuroimage.2024.120551

Chen, J., Müller, V. I., Dukart, J., Hoffstaedter, F., Baker, J. T., Holmes, A. J., Vatansever, D., Nickl-Jockschat, T., Liu, X., Derntl, B., Kogler, L., Jardri, R., Gruber, O., Aleman, A., Sommer, I. E., Eickhoff, S. B., & Patil, K. R. (2021). Intrinsic connectivity patterns of task-defined brain networks Allow Individual Prediction of Cognitive Symptom Dimension of Schizophrenia and Are Linked to Molecular Architecture. *Biological Psychiatry*, 89(3), 308–319. https://doi.org/10.1016/j.biopsych.2020.09.024

Chen, P., Ye, E., Jin, X., Zhu, Y., & Wang, L. (2019). Association between thalamocortical functional connectivity abnormalities and cognitive deficits in schizophrenia. *Scientific Reports*, 9(1), 2952. https://doi.org/10.1038/s41598-019-39367-z

Choi, J.-S., Kang, D.-H., Kim, J.-J., Ha, T.-H., Roh, K. S., Youn, T., & Kwon, J. S. (2005). Decreased caudal anterior cingulate gyrus volume and positive symptoms in schizophrenia. *Psychiatry Research*, 139(3), 239–247. https://doi.org/10.1016/j.pscychresns.2004.05.008

Costa, R. Q. M. da, Porto, F. H. de G., & Marrocos, R. P. (2013). Dissociation of depression from apathy in traumatic brain injury: A case report. *Dementia & Neuropsychologia*, 7, 312–315. https://doi.org/10.1590/s1980-57642013dn70300014

de Filippis, R., Carbone, E. A., Gaetano, R., Bruni, A., Pugliese, V., Segura-Garcia, C., & De Fazio, P. (2019). Machine learning techniques in a structural and functional MRI diagnostic approach in schizophrenia: A systematic review. *Neuropsychiatric Disease and Treatment*, 15, 1605–1627. https://doi.org/10.2147/ndt.s20241

Dong, D., Wang, Y., Chang, X., Luo, C., & Yao, D. (2018). Dysfunction of large-scale brain networks in schizophrenia: A meta-analysis of resting-state functional connectivity. *Schizophrenia Bulletin*, 44(1), 168–181. https://doi.org/10.1093/schbul/sbx034

Elliott, M. L., Knodt, A. R., & Hariri, A. R. (2021). Striving toward translation: Strategies for reliable fMRI measurement. *Trends in Cognitive Sciences*, 25(9), 776–787. https://doi.org/10.1016/j.tics.2021.05.008

Fan, L., Li, H., Zhuo, J., Zhang, Y., Wang, J., Chen, L., Yang, Z., Chu, C., Xie, S., Laird, A. R., Fox, P. T., Eickhoff, S. B., Yu, C., & Jiang, T. (2016). The human brainnetome atlas: A new brain atlas based on connectional architecture. *Cerebral Cortex*, 26(8), 3508–3526. https://doi.org/10.1093/cercor/bhw157

Fan, Y.-S., Li, H., Guo, J., Pang, Y., Li, L., Hu, M., Li, M., Wang, C., Sheng, W., Liu, H., Gao, Q., Chen, X., Zong, X., & Chen, H. (2022). Tracking positive and negative symptom improvement in first-episode schizophrenia treated with risperidone using individual-level functional connectivity. *Brain Connectivity*, 12(5), 454–464. https://doi.org/10.1089/brain.2021.0061

Fan, Y., Li, L., Peng, Y., Li, H., Guo, J., Li, M., Yang, S., Yao, M., Zhao, J., Liu, H., Liao, W., Guo, X., Han, S., Cui, Q., Duan, X., Xu, Y., Zhang, Y., & Chen, H. (2021). Individual-specific functional connectome biomarkers predict schizophrenia positive symptoms during adolescent brain maturation. *Human Brain Mapping*, 42(5), 1475–1484. https://doi.org/10.1002/hbm.25307

Feng, A., Luo, N., Zhao, W., Calhoun, V. D., Jiang, R., Zhi, D., Shi, W., Jiang, T., Yu, S., Xu, Y., Liu, S., & Sui, J. (2022). Multimodal brain deficits shared in early-onset and adult-onset schizophrenia predict positive symptoms regardless of illness stage. *Human Brain Mapping*, 43(11), 3486–3497. https://doi.org/10.1002/hbm.25862

Ferri, J., Ford, J. M., Roach, B. J., Turner, J. A., van Erp, T. G., Voyvodic, J., Preda, A., Belger, A., Bustillo, J., O'Leary, D., Mueller, B. A., Lim, K. O., McEwen, S. C., Calhoun, V. D., Diaz, M., Glover, G., Greve, D., Wible, C. G., Vaidya, J. G., … Mathalon, D. H. (2018). Resting-state thalamic dysconnectivity in schizophrenia and relationships with symptoms. *Psychological Medicine*, 48(15), 2492–2499. https://doi.org/10.1017/s003329171800003x

Guo, L., Ma, J., Cai, M., Zhang, M., Xu, Q., Wang, H., Zhang, Y., Yao, J., Sun, Z., Chen, Y., Xue, H., Zhang, Y., Wang, S., Xue, K., Zhu, D., & Liu, F. (2023). Transcriptional signatures of the whole-brain voxel-wise resting-state functional network centrality alterations in schizophrenia. *Schizophrenia (Heidelberg, Germany)*, 9(1), 87. https://doi.org/10.1038/s41537-023-00422-4

Jiang, R., Calhoun, V. D., Fan, L., Zuo, N., Jung, R., Qi, S., Lin, D., Li, J., Zhuo, C., Song, M., Fu, Z., Jiang, T., & Sui, J. (2020). Gender differences in connectome-based predictions of individualized intelligence

quotient and sub-domain scores. *Cerebral Cortex*, *30*(3), 888–900. https://doi.org/10.1093/cercor/bhz134

Jiang, R., Calhoun, V. D., Noble, S., Sui, J., Liang, Q., Qi, S., & Scheinost, D. (2023). A functional connectome signature of blood pressure in >30 000 participants from the UK biobank. *Cardiovascular Research*, *119*(6), 1427–1440. https://doi.org/10.1093/cvr/cvac116

Jiang, R., Calhoun, V. D., Zuo, N., Lin, D., Li, J., Fan, L., Qi, S., Sun, H., Fu, Z., Song, M., Jiang, T., & Sui, J. (2018). Connectome-based individualized prediction of temperament trait scores. *Neuroimage*, *183*, 366–374. https://doi.org/10.1016/j.neuroimage.2018.08.038

Jiang, R., Scheinost, D., Zuo, N., Wu, J., Qi, S., Liang, Q., Zhi, D., Luo, N., Chung, Y., Liu, S., Xu, Y., Sui, J., & Calhoun, V. (2022). A neuroimaging signature of cognitive aging from whole-brain functional connectivity. *Advanced Science*, *9*(24), 2201621. https://doi.org/10.1002/advs.202201621

Jiang, R., Woo, C.-W., Qi, S., Wu, J., & Sui, J. J. (2022). Interpreting brain biomarkers: Challenges and solutions in interpreting machine learning-based predictive neuroimaging. *IEEE Signal Processing Magazine*, *39*(4), 107–118. https://doi.org/10.1109/msp.2022.3155951

Jiang, R., Zuo, N., Ford, J. M., Qi, S., Zhi, D., Zhuo, C., Xu, Y., Fu, Z., Bustillo, J., Turner, J. A., Calhoun, V. D., & Sui, J. (2020). Task-induced brain connectivity promotes the detection of individual differences in brain-behavior relationships. *Neuroimage*, *207*, 116370. https://doi.org/10.1016/j.neuroimage.2019.116370

Joyce, E. M., & Roiser, J. P. (2007). Cognitive heterogeneity in schizophrenia. *Current Opinion in Psychiatry*, *20*(3), 268–272. https://doi.org/10.1097/YCO.0b013e3280ba4975

Kaur, A., Basavanagowda, D. M., Rathod, B., Mishra, N., Fuad, S., Nosher, S., Alrashid, Z. A., Mohan, D., & Heindl, S. E. (2020). Structural and functional alterations of the temporal lobe in schizophrenia: A literature review. *Cureus*, *12*(10), 11177. https://doi.org/10.7759/cureus.11177

Kay, S. R., Fiszbein, A., & Opler, L. A. (1987). The positive and negative syndrome scale (PANSS) for schizophrenia. *Schizophrenia Bulletin*, *13*(2), 261–276. https://doi.org/10.1093/schbul/13.2.261

Kraguljac, N. V., McDonald, W. M., Widge, A. S., Rodriguez, C. I., Tohen, M., & Nemeroff, C. B. (2021). Neuroimaging biomarkers in schizophrenia. *The American Journal of Psychiatry*, *178*(6), 509–521. https://doi.org/10.1176/appi.ajp.2020.20030340

Lesh, T. A., Tanase, C., Geib, B. R., Niendam, T. A., Yoon, J. H., Minzenberg, M. J., Ragland, J. D., Solomon, M., & Carter, C. S. (2015). A multimodal analysis of antipsychotic effects on brain structure and function in first-episode schizophrenia. *JAMA Psychiatry*, *72*(3), 226–234. https://doi.org/10.1001/jamapsychiatry.2014.2178

Li, H., Xu, Y., Zhang, K., Hoptman, M. J., & Zuo, X. (2015). Homotopic connectivity in drug-naïve, first-episode, early-onset schizophrenia. *Journal of Child Psychology and Psychiatry*, *56*(4), 432–443. https://doi.org/10.1111/jcpp.12307

Li, Y., Li, W., Xie, D., Wang, Y., Cheung, E. F. C., & Chan, R. C. K. (2018). Grey matter reduction in the caudate nucleus in patients with persistent negative symptoms: An ALE meta-analysis. *Schizophrenia Research*, *192*, 9–15. https://doi.org/10.1016/j.schres.2017.04.005

Liang, C., Pearlson, G., Bustillo, J., Kochunov, P., Turner, J. A., Wen, X., Jiang, R., Fu, Z., Zhang, X., Li, K., Xu, X., Zhang, D., Qi, S., & Calhoun, V. D. (2023). Psychotic symptom, mood, and cognition-associated multimodal MRI reveal shared links to the salience network within the psychosis spectrum disorders. *Schizophrenia Bulletin*, *49*(1), 172–184. https://doi.org/10.1093/schbul/sbac158

Liu, W., & Li, Q. (2017). An efficient elastic net with regression coefficients method for variable selection of spectrum data. *PLoS One*, *12*(2), e0171122. https://doi.org/10.1371/journal.pone.0171122

Luck, D., Danion, J.-M., Marrer, C., Pham, B.-T., Gounot, D., & Foucher, J. (2010). The right parahippocampal gyrus contributes to the formation and maintenance of bound information in working memory. *Brain and Cognition*, *72*(2), 255–263. https://doi.org/10.1016/j.bandc.2009.09.009

McIntosh, A., Bookstein, F., Haxby, J. V., & Grady, C. L. (1996). Spatial pattern analysis of functional brain images using partial least squares. *Neuroimage*, *3*(3), 143–157. https://doi.org/10.1006/nimg.1996.0016

Meskaldji, D.-E., Preti, M. G., Bolton, T. A., Montandon, M.-L., Rodriguez, C., Morgenthaler, S., Giannakopoulos, P., Haller, S., & Van De Ville, D. (2016). Prediction of long-term memory scores in MCI based on resting-state fMRI. *NeuroImage: Clinical*, *12*, 785–795. https://doi.org/10.1016/j.nicl.2016.10.004

Mwansisya, T. E., Hu, A., Li, Y., Chen, X., Wu, G., Huang, X., Lv, D., Li, Z., Liu, C., Xue, Z., Feng, J., & Liu, Z. (2017). Task and resting-state fMRI studies in first-episode schizophrenia: A systematic review. *Schizophrenia Research*, *189*, 9–18. https://doi.org/10.1016/j.schres.2017.02.026

Nguyen, D. V., & Rocke, D. M. (2002). Tumor classification by partial least squares using microarray gene expression data. *Bioinformatics*, *18*(1), 39–50. https://doi.org/10.1093/bioinformatics/18.1.39

Perez-Rando, M., Elvira, U. K. A., García-Martí, G., Gadea, M., Aguilar, E. J., Escarti, M. J., Ahulló-Fuster, M. A., Grasa, E., Corripio, I., Sanjuan, J., & Nacher, J. (2022). Alterations in the volume of thalamic nuclei in patients with schizophrenia and persistent auditory hallucinations. *NeuroImage: Clinical*, *35*, 103070. https://doi.org/10.1016/j.nicl.2022.103070

Pettersson-Yeo, W., Allen, P., Benetti, S., McGuire, P., & Mechelli, A. J. (2011). Dysconnectivity in schizophrenia: Where are we now? *Neuroscience & Biobehavioral Reviews*, *35*(5), 1110–1124. https://doi.org/10.1017/s003329171800003x

Qi, S., Bustillo, J., Turner, J. A., Jiang, R., Zhi, D., Fu, Z., Deramus, T. P., Vergara, V., Ma, X., Yang, X., Stevens, M., Zhuo, C., Xu, Y., Calhoun, V. D., & Sui, J. (2020). The relevance of transdiagnostic shared networks to the severity of symptoms and cognitive deficits in schizophrenia: A multimodal brain imaging fusion study. *Translational Psychiatry*, *10*(1), 149. https://doi.org/10.1038/s41398-020-0834-6

Qi, S., Schumann, G., Bustillo, J., Turner, J. A., Jiang, R., Zhi, D., Fu, Z., Mayer, A. R., Vergara, V. M., Silva, R. F., Iraji, A., Chen, J., Damaraju, E., Ma, X., Yang, X., Stevens, M., Mathalon, D. H., Ford, J. M., Voyvodic, J., ... Whelan, R. (2021). Reward Processing in Novelty Seekers: A Transdiagnostic Psychiatric Imaging Biomarker. *Biological Psychiatry*, *90*(8), 529–539. https://doi.org/10.1016/j.biopsych.2021.01.011

Qi, S., Sui, J., Pearlson, G., Bustillo, J., Perrone-Bizzozero, N. I., Kochunov, P., Turner, J. A., Fu, Z., Shao, W., Jiang, R., Yang, X., Liu, J., Du, Y., Chen, J., Zhang, D., & Calhoun, V. D. (2022). Derivation and utility of schizophrenia polygenic risk associated multimodal MRI frontotemporal network. *Nature Communications*, *13*(1), 4929. https://doi.org/10.1038/s41467-022-32513-8

Qiu, X., Lu, S., Zhou, M., Yan, W., Du, J., Zhang, A., Xie, S., & Zhang, R. (2021). The relationship between abnormal resting-state functional connectivity of the left superior frontal gyrus and cognitive impairments in youth-onset drug-naïve schizophrenia. *Frontiers in Psychiatry*, *12*, 679642. https://doi.org/10.3389/fpsyt.2021.679642

Raimondo, L., Oliveira Ícaro A. F., Heij, J., Priovoulos, N., Kundu, P., Leoni, R. F., & van der Zwaag, W. (2021). Advances in resting state fMRI acquisitions for functional connectomics. *Neuroimage*, *243*, 118503. https://doi.org/10.1016/j.neuroimage.2021.118503

Rodrigues-Amorim, D., Rivera-Baltanás, T., López, M., Spuch, C., Olivares, J. M., & Agís-Balboa, R. C. (2017). Schizophrenia: A review of potential biomarkers. *Journal of Psychiatric Research*, *93*, 37–49. https://doi.org/10.1016/j.jpsychires.2017.05.009

Shen, X., Finn, E. S., Scheinost, D., Rosenberg, M. D., Chun, M. M., Papademetris, X., & Constable, R. T. J. (2017). Using connectome-based predictive modeling to predict individual behavior from brain connectivity. *Nature Protocols*, *12*(3), 506–518. https://doi.org/10.1038/nprot.2016.178

Silbersweig, D. A., Stern, E., Frith, C., Cahill, C., Holmes, A., Grootoonk, S., Seaward, J., McKenna, P., Chua, S. E., Schnorr, L., Jones, T., & Frackowiak, R. S. J. (1995). A functional neuroanatomy of hallucinations in schizophrenia. *Nature*, *378*(6553), 176–179. https://doi.org/10.1038/378176a0

Skudlarski, P., Jagannathan, K., Anderson, K., Stevens, M. C., Calhoun, V. D., Skudlarska, B. A., & Pearlson, G. J. (2010). Brain connectivity is not only lower but different in schizophrenia: A combined anatomical and functional approach. *Biological Psychiatry*, *68*(1), 61–69. https://doi.org/10.1016/j.biopsych.2010.03.035

Sui, J., Qi, S., van Erp, T. G. M., Bustillo, J., Jiang, R., Lin, D., Turner, J. A., Damaraju, E., Mayer, A. R., Cui, Y., Fu, Z., Du, Y., Chen, J., Potkin, S. G., Preda, A., Mathalon, D. H., Ford, J. M., Voyvodic, J., Mueller, B. A., ... Calhoun, V. D. (2018). Multimodal neuromarkers in schizophrenia via cognition-guided MRI fusion. *Nature Communications*, *9*(1), 3028. https://doi.org/10.1038/s41467-018-05432-w

Sun, H., Jiang, R., Qi, S., Narr, K. L., Wade, B. S., Upston, J., Espinoza, R., Jones, T., Calhoun, V. D., Abbott, C. C., & Sui, J. (2020). Preliminary prediction of individual response to electroconvulsive therapy using whole-brain functional magnetic resonance imaging data. *NeuroImage: Clinical*, *26*, 102080. https://doi.org/10.1016/j.nicl.2019.102080

Tang, Y., Wang, L., Cao, F., & Tan, L. (2012). Identify schizophrenia using resting-state functional connectivity: An exploratory research and analysis. *Biomedical Engineering Online*, *11*, 50. https://doi.org/10.1186/1475-925x-11-50

Uscătescu, L. C., Kronbichler, L., Stelzig-Schöler, R., Pearce, B.-G., Said-Yürekli, S., Reich, L. A., Weber, S., Aichhorn, W., & Kronbichler, M. (2021). Effective connectivity of the hippocampus can differentiate patients with schizophrenia from healthy controls: A spectral DCM approach. *Brain Topography*, *34*, 762–778. https://doi.org/10.1007/s10548-021-00868-8

Venkataraman, A., Whitford, T. J., Westin, C.-F., Golland, P., & Kubicki, M. J. (2012). Whole brain resting state functional connectivity abnormalities in schizophrenia. *Schizophrenia Research*, *139*(1–3), 7–12.

Wang, D., Li, M., Wang, M., Schoeppe, F., Ren, J., Chen, H., Öngür, D., Brady, R. O., Baker, J. T., & Liu, H. (2020). Individual-specific functional connectivity markers track dimensional and categorical features of psychotic illness. *Molecular Psychiatry*, *25*(9), 2119–2129. https://doi.org/10.1038/s41380-018-0276-1

Weiner, K. S., & Grill-Spector, K. (2013). Neural representations of faces and limbs neighbor in human high-level visual cortex: Evidence for a new organization principle. *Psychological Research*, *77*(1), 74–97. https://doi.org/10.1007/s00426-011-0392-x

Xi, Y.-B., Guo, F., Liu, W.-M., Fu, Y.-F., Li, J.-M., Wang, H.-N., Chen, F.-L., Cui, L.-B., Zhu, Y.-Q., Li, C., Kang, X.-W., Li, B.-J., & Yin, H. (2021). Triple network hypothesis-related disrupted connections in schizophrenia: A spectral dynamic causal modeling analysis with functional magnetic resonance imaging. *Schizophrenia Research*, *233*, 89–96. https://doi.org/10.1016/j.schres.2021.06.024

Yamaguchi, H., Hashimoto, Y., Sugihara, G., Miyata, J., Murai, T., Takahashi, H., Honda, M., Hishimoto, A., & Yamashita, Y. (2021). Three-dimensional convolutional autoencoder extracts features of structural brain images with a "diagnostic label-free" approach: Application to schizophrenia datasets. *Frontiers in Neuroscience*, *15*, 652987.

Yoo, K., Rosenberg, M. D., Hsu, W.-T., Zhang, S., Li, C.-S. R., Scheinost, D., Constable, R. T., & Chun, M. M. (2018). Connectome-based predictive modeling of attention: Comparing different functional connectivity features and prediction methods across datasets. *Neuroimage*, *167*, 11–22.

Zeng, J., Zhang, W., Wu, G., Wang, X., Shah, C., Li, S., Xiao, Y., Yao, L., Cao, H., Li, Z., Sweeney, J. A., Lui, S., & Gong, Q. (2022). Effects of antipsychotic medications and illness duration on brain features that distinguish schizophrenia patients. *Schizophrenia Bulletin*, *48*(6), 1354–1362. https://doi.org/10.1093/schbul/sbac094

Zhao, J., Zhang, Y., Liu, F., Chen, J., Zhao, J., & Guo, W. (2022). Abnormal global-brain functional connectivity and its relationship with cognitive deficits in drug-naive first-episode adolescent-onset schizophrenia. *Brain Imaging and Behavior*, *16*(3), 1303–1313. https://doi.org/10.1007/s11682-021-00597-3

Zheng, J., Wei, X., Wang, J., Lin, H., Pan, H., & Shi, Y. (2021). Diagnosis of schizophrenia based on deep learning using fMRI. *Computational and Mathematical Methods in Medicine*, *2021*, 8437260. https://doi.org/10.1155/2021/8437260

SUPPORTING INFORMATION

Additional supporting information can be found online in the Supporting Information section at the end of this article.